EMBO reports

scientific report

The supramolecular architecture of junctional microdomains in native lens membranes

Nikolay Buzhynskyy[1], Richard K Hite[2], Thomas Walz[2] & Simon Scheuring[1+]

[1]Institut Curie, UMR168-CNRS, Paris, France, and [2]Department of Cell Biology, Harvard Medical School, Boston, Massachusetts, USA

Gap junctions formed by connexons and thin junctions formed by lens-specific aquaporin 0 (AQP0) mediate the tight packing of fibre cells necessary for lens transparency. Gap junctions conduct water, ions and metabolites between cells, whereas junctional AQP0 seems to be involved in cell adhesion. High-resolution atomic force microscopy (AFM) showed the supramolecular organization of these proteins in native lens core membranes, in which AQP0 forms two-dimensional arrays that are surrounded by densely packed gap junction channels. These junctional microdomains simultaneously provide adhesion and communication between fibre cells. The AFM topographs also showed that the extracellular loops of AQP0 in junctional microdomains adopt a conformation that closely resembles the structure of junctional AQP0, in which the water pore is thought to be closed. Finally, time-lapse AFM imaging provided insights into AQP0 array formation. This first high-resolution view of a multicomponent eukaryotic membrane shows how membrane proteins self-assemble into functional microdomains.

Keywords: aquaporin; atomic force microscopy; connexin; gap junction; membrane protein

EMBO reports (2007) **8**, 51–55. doi:10.1038/sj.embor.7400858

INTRODUCTION

The lens of the eye has developed some remarkable adaptations that ensures its transparency (Donaldson *et al*, 2001). To minimize light scattering the lens is avascular, and fibre cells degrade organelles during differentiation. In addition, fibre cells are tightly packed to cause intercellular distances to be smaller than the wavelength of visible light. Two types of membrane proteins form junctions between fibre cells: aquaporin 0 (AQP0) and connexins (Zampighi *et al*, 1982). Gap junctions are cell-to-cell channels with pores large enough to allow the passage of metabolites and ions (Kumar & Gilula, 1996). By contrast, the main function of AQP0 in thin junctions seems to be cell adhesion (Gonen *et al*, 2005). Mutations in both proteins result in the formation of a cataract (Shiels & Bassnett, 1996; Harris, 2001).

Aquaporins form a large family of membrane pores that conduct only water or small, uncharged solutes (Agre, 2004). Although the lens-specific AQP0 is a poor water pore when compared with the more efficient AQP1 (Chandy *et al*, 1997), it is the most abundant protein in fibre cells accounting for approximately 50% of the total membrane protein content (Alcala *et al*, 1975). AQP0 is present in nonjunctional membranes, where it forms water pores, and in thin junctions between fibre cells, where structural evidence suggests that it no longer conducts water (Gonen *et al*, 2004a). Atomic resolution structures have been determined for both nonjunctional, open AQP0 (Harries *et al*, 2004) and junctional, closed AQP0 (Gonen *et al*, 2004a). Nonjunctional AQP0 is converted to junctional AQP0 by proteolysis of the cytoplasmic amino and carboxyl termini (Gonen *et al*, 2004b), which occurs as fibre cells mature and become part of the lens core that is surrounded by younger fibre cells of the lens cortex (Takemoto *et al*, 1986).

Connexins (Cx43, Cx44 and Cx49 in the sheep lens, homologous to human Cx43, Cx45 and Cx50, respectively) are the second most abundant proteins in fibre cells, constituting more than 10% of the total membrane protein content (Fleschner & Cenedella, 1991). Six connexins form a connexon or half-channel, and docking of two connexons from adjacent cells creates a cell-to-cell gap junction channel (Kumar & Gilula, 1996). Gap junctions are important in ion and metabolite flux between neighbouring cells and in cell-to-cell signalling. Electron crystallography has been used to produce a sub-nanometer resolution density map of the recombinant cardiac gap junction (Unger *et al*, 1999), which formed the basis for a hypothetical Cα model of the transmembrane α-helices (Fleishman *et al*, 2004).

The atomic force microscope (AFM; Binnig *et al*, 1986) has been developed into a powerful tool for studying biological membranes. By using AFM, topographs can be obtained at approximately 10 Å resolution from two-dimensional (2D) crystallized membrane proteins (Müller *et al*, 1999). Recently, high-resolution images showed the supramolecular assemblies of membrane proteins within native membranes (Scheuring & Sturgis, 2005).

[1]Institut Curie, UMR168-CNRS, 26 Rue d'Ulm, 75248 Paris, France
[2]Department of Cell Biology, Harvard Medical School, 240 Longwood Avenue, Boston, Massachusetts 02115, USA
[+]Corresponding author. Tel: +33 1 42 34 67 81; Fax: +33 1 40 51 06 36;
E-mail: simon.scheuring@curie.fr

Received 24 July 2006; revised 13 October 2006; accepted 16 October 2006; published online 24 November 2006

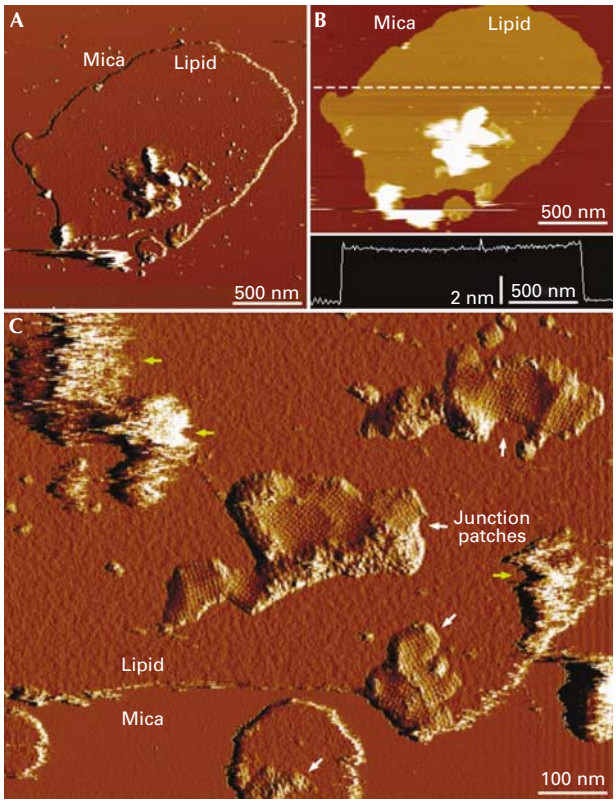

Fig 1 | Junctional microdomains within planar lipid bilayers. (**A**) Deflection and (**B**) height image of a native membrane patch isolated from the lens core. The height profile along the dashed line in (**B**) is shown in the lower panel and shows that the thickness of the bilayer is 46 Å. (**C**) Removal of vesicular structures that were attached to the membrane patches (yellow arrows) with the AFM tip showed the presence of corrugated patches that protruded from the lipid bilayer (white arrows). The patches contained square aquaporin 0 arrays.

RESULTS

Lens membranes contain junctional microdomains

We used high-resolution AFM to analyse the organization of AQP0 and connexons in native membranes isolated from the lens core. The observed membrane patches were often larger than 2 μm in diameter (Fig 1A). Over large areas, the membranes had a thickness of 46 ± 2 Å ($n = 50$) and showed smooth surfaces (Fig 1B), as described previously for planar lipid bilayers (Giocondi & Le Grimellec, 2004). Often, material was attached to the membrane patches, which could be removed with the AFM tip, uncovering corrugated patches protruding from the bilayer surface (Fig 1C). The patches contained square arrays, which had an average height of approximately 1 nm above the lipid surface. As these arrays are characteristic of junctional AQP0 (Zampighi *et al*, 1982), the material that was removed was probably membrane containing AQP0 that formed junctions with the adsorbed membrane patches. Removal of membranes with the AFM has previously been reported for both isolated hepatic gap junctions (Hoh *et al*, 1991) and double-layered AQP0 2D crystals (Fotiadis *et al*, 2000).

The AQP0 arrays ranged in size from only a few assembled tetramers to arrays more than 500 nm in diameter. The packing of AQP0 tetramers in the 2D arrays in native membranes (Fig 2A; $a = b = 65 \pm 2$ Å, $\gamma = 90 \pm 2$; $n = 69$) is the same as the lattice parameters in double-layered 2D crystals (Fotiadis *et al*, 2000), providing evidence that structural information gained from electron crystallography of double-layered AQP0 2D crystals (Gonen *et al*, 2005) is representative of the native situation.

Time-lapse imaging of array borders provided insight into the assembly of AQP0 arrays at the molecular level (Fig 2B). AQP0 tetramers in the centre of the 2D array were aligned with the crystal lattice. However, the first few rows on the array edge showed defects, such as tetramers that were displaced from their lattice positions. When the same area was imaged again 1 min later, these tetramers were found at their optimal lattice positions (Fig 2B, indicated by arrows). Similarly, shifts between adjacent rows of tetramers in the lattice also disappeared with time.

AQP0 in arrays is in the junctional conformation

Removal of the top membrane with the AFM tip allowed us to record high-resolution topographs of the extracellular surface of AQP0, in which individual surface loops were resolved. Unsymmetrized (Fig 2C) and four-fold symmetrized (Fig 2D) averages showed three protrusions per monomer: two on the periphery (labelled C_1 and C_2 in Fig 2D) and a smaller one close to the tetramer centre (labelled A in Fig 2D). Comparison of the experimental topography (Fig 2D) with surface representations of the atomic structures of the junctional water pore (Gonen *et al*, 2005; Fig 2E) and the nonjunctional water pore (Harries *et al*, 2004; Fig 2F) identified protrusion C_1 as the start of extracellular loop C (residues Pro 109, Pro 110, Ala 111 and Val 112), and protrusion C_2 as the end of loop C (residues His 122, Pro 123, Gly 124 and Val 125). The third protrusion close to the centre of the tetramer represents the extracellular loop A (residues Ala 35, Pro 36, Gly 37 and Pro 38). This loop is positioned differently in junctional (labelled A in Fig 2E; Gonen *et al*, 2005) and nonjunctional AQP0 (labelled A′ in Fig 2F; Harries *et al*, 2004). We found a good fit of the observed central protrusion with the position of loop A in junctional AQP0 (white circle A in Fig 2D), whereas no protrusion was detected at the position of loop A in nonjunctional AQP0 (red circle A′ in Fig 2D).

AQP0 arrays are surrounded by connexons

AFM images of native lens membranes showed that many AQP0 arrays were surrounded by strongly corrugated patches that protruded further from the membrane than AQP0 (Figs 1C,3A). Images at higher magnification showed that these regions consist of flower-shaped particles with a height of approximately 2.5 nm above the lipid surface (Fig 3B). Unsymmetrized (Fig 3D, left) and six-fold symmetrized (Fig 3D, right) connexon averages consisted of six subunits with an outer diameter of approximately 80 Å and a top diameter of approximately 40 Å surrounding a central cavity of approximately 20 Å. These dimensions are consistent with those of connexons (Unger *et al*, 1999). Patches of densely packed connexons surrounded AQP0 arrays and separated neighbouring AQP0 arrays with different orientations (Fig 3A, arrows). The connexon domains that we observed ranged from a single row to an array approximately 50 nm in width. Connexons that terminate the AQP0 arrays by a single row seem to be composed of Cx44 and Cx49, as—in the human lens—Cx45 directly and Cx50 indirectly interact with AQP0 (Fig 3B, arrows; Yu *et al*, 2005). An

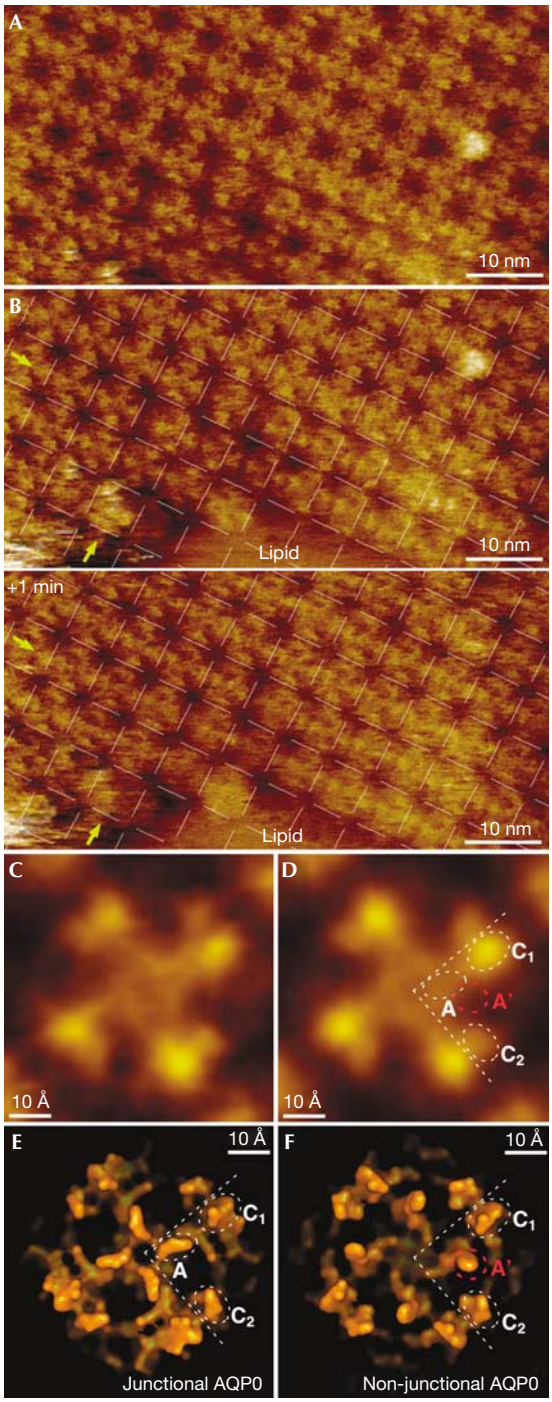

Fig 2 | Characterization of aquaporin 0 two-dimensional arrays. (**A**) High-resolution atomic force microscopy topograph of an aquaporin 0 (AQP0) array. (**B**) Time-lapse imaging of the border region of the same array with 1-min time interval (the AQP0 2D lattice is superimposed in both panels). AQP0 tetramers adjust to their lattice positions with time, as seen in the two edge rows of the array. Some tetramers move half a unit cell between the two images (indicated by arrows). (**C**) Unsymmetrized and (**D**) four-fold symmetrized AQP0 tetramer average topographs. (**E**) Surface representation of the junctional and (**F**) nonjunctional conformation of the extracellular AQP0 surface, which differ in the position of loop A.

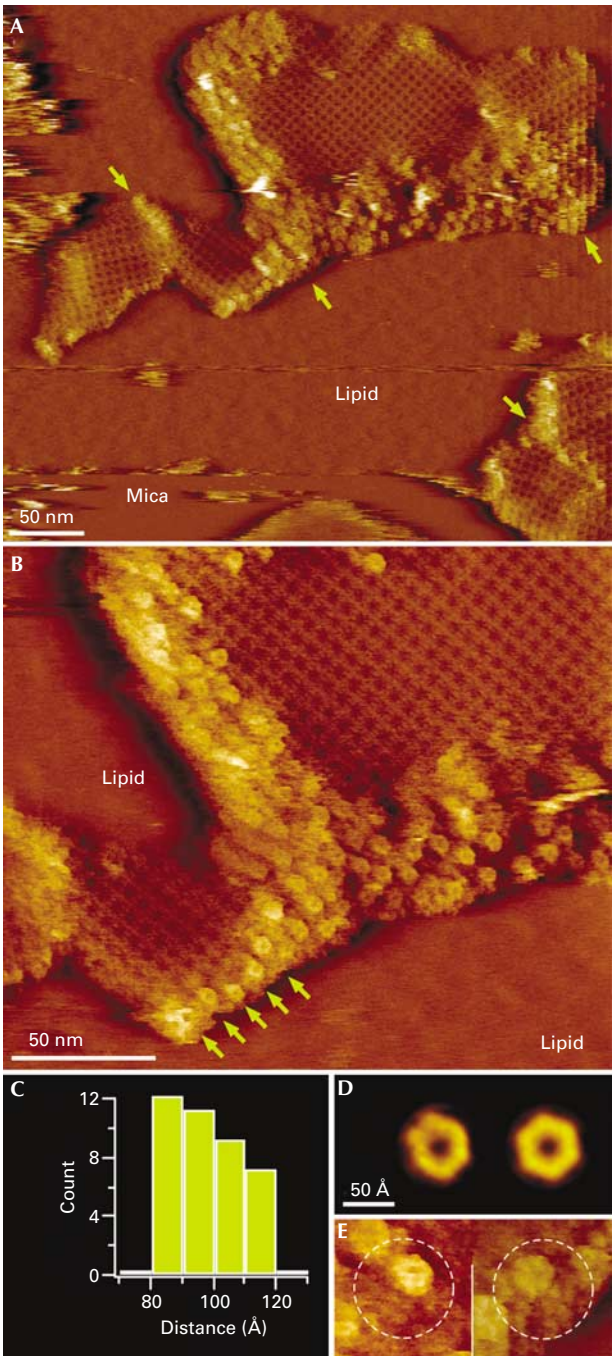

Fig 3 | High-resolution analysis of an aquaporin 0–connexon microdomain. (**A**) Topograph of aquaporin 0 (AQP0) arrays surrounded and separated (arrows) by densely packed connexon patches. (**B**) A higher magnification topograph that shows the characteristic flower shape of the connexons. The arrows indicate a row of connexons terminating an AQP0 array. (**C**) Histogram of distances between neighbouring connexons. (**D**) Unsymmetrized (left) and six-fold symmetrized connexon average topographies, calculated from 49 molecules. (**E**) AQP0–connexon pairs within unordered regions surrounding crystalline AQP0 arrays. In the left panel, the connexon is at the top right and AQP0 is at the bottom left of the circled area; in the right panel, the connexon is at the top left and AQP0 is at the bottom right of the circled area.

analysis of centre-to-centre distances between neighbouring connexons showed a peak (~30%, $n=40$) between 80 Å and 90 Å (Fig 3C). This is similar to the distance of 77 Å between connexons in 2D crystals (Unger *et al*, 1999), suggesting that this fraction represents connexons that are in contact. Although a fraction of connexons packed very densely, they never formed hexagonal lattices, a known difference between gap junctions in the lens and other tissues (Kistler *et al*, 1994). The average centre-to-centre distance was 96 ± 12 Å and the largest distance measured between connexons in a patch was 120 Å. Individual connexons must therefore be separated by lipids and/or other proteins; indeed individual AQP0 tetramers could be seen interspersed among connexons (Fig 3E).

DISCUSSION

By using our AFM images of native lens membranes, we present the first high-resolution view of the organization of a multi-component eukaryotic membrane. We find that AQP0 and connexons organize in junctional microdomains within large planar lipid bilayers (Fig 1). Time-lapse imaging suggests that AQP0 arrays assemble in a two-step process. First, AQP0 tetramers diffusing in the lipid bilayer are captured by existing arrays. The numerous defects in the outermost rows of the lattice suggest that initial interactions between newly recruited tetramers and AQP0 arrays are weak. A weak interaction between AQP0 is consistent with the finding that AQP0 arrays are held together almost exclusively by protein–lipid interactions (Gonen *et al*, 2005). Second, tetramers arrange at array boarders to achieve optimal alignment to the crystal packing (Fig 2A).

Why do individual AQP0 tetramers associate with preformed arrays and why does AQP0 organize in domains that cover less than 10% of the total area (Fig 1) rather than diffusing over the entire membrane? Hydrophobic mismatch (Jensen & Mouritsen, 2004) is the most likely driving force for AQP0 assembly. In 2D crystals, the lipid bilayer formed by dimyristoyl phosphatidyl choline surrounding the AQP0 tetramers has a thickness of approximately 34 Å from phosphate to phosphate (Gonen *et al*, 2005), whereas AFM measured a thickness of 46 Å for the lipid bilayer outside junctions (Fig 1B). The hydrophobic length of the transmembrane domain of AQP0 thus seems to be shorter than the hydrophobic thickness of the fibre cell membrane. Such a hydrophobic mismatch is energetically unfavourable and would provide a driving force for AQP0 self-assembly.

The juxtaposition of AQP0 thin junctions and connexin gap junctions has been described in thin sections through the lens (Zampighi *et al*, 1982). Another study reported that the C terminus of AQP0 directly interacts with the chick orthologue of Cx50 (Yu *et al*, 2005). A freeze-fracture and immunolabelling study indicate that AQP0 coexists with connexons in the lens cortex in the so-called 'mixed junctions' (Zampighi *et al*, 2002). Although the freeze-fracture studies did not show any particular organization of these microdomains in young fibre cells, we found that, in mature lens core fibre cells, they are composed of AQP0 arrays surrounded by connexons within lipid bilayers. In the cortex, AQP0 is largely full-length, suggesting association of AQP0 and connexons over the AQP0 C terminus. In the core, the N and C termini of AQP0 are cleaved, suggesting that the mixed junctional microdomains remain stable and no longer depend on such AQP0–connexon interactions.

The topography of loop A compared more favourably with the structure of junctional AQP0 (Gonen *et al*, 2005) than with the nonjunctional conformation (Harries *et al*, 2004). As the interacting AQP0 array was removed by the AFM tip (Fig 1), the finding of loop A being in the junctional conformation, without a covering AQP0 array, corroborates that the conformation of loop A is caused by cleavage of the cytoplasmic termini and is not a result of junction formation (Gonen *et al*, 2004b). The fact that loop A protrudes less in the topography than expected from the atomic model might reflect flexibility of the loop, subjected to a loading force applied by the AFM tip.

The structure of junctional AQP0 suggests that the water pores are closed (Gonen *et al*, 2004b). The structural resemblance between AQP0 in native membranes and the junctional structure suggests that the pores are also closed in AQP0–connexon microdomains; however, this is more than compensated for by the many gap junctions surrounding AQP0. The organization of AQP0 and connexons in junctional microdomains minimizes the distances between fibre cells through the extended AQP0 arrays while assuring sufficient exchange of solutes between cells through the surrounding gap junctions.

METHODS

Lens fibre cell membranes. Sheep lenses were dissected to remove the soft cortical tissue and membranes were prepared from the hard lens core according to Gonen *et al* (2004b).

Atomic force microscopy. Mica supports were immersed in 40 µl adsorption buffer (10 mM Tris–HCl, pH 7.2, 150 mM KCl, 25 mM $MgCl_2$). Then 3 µl of lens membrane solution was injected into the buffer drop. After approximately 1 h, the sample was rinsed with recording buffer (10 mM Tris–HCl, pH 7.2, 150 mM KCl). The AFM was operated in contact mode at ambient temperature and pressure. Imaging was carried out with a commercial Nanoscope-E AFM (Veeco, Santa Barbara, CA, USA) equipped with a 160-µm scanner (J-scanner) and oxide-sharpened Si_3N_4 cantilevers (length 100 µm; $k=0.09$ N/m; Olympus Ltd, Tokyo, Japan). For imaging, minimal loading forces of approximately 100 pN were applied, at scan frequencies of 4–7 Hz, using optimized feedback parameters. Time-lapse imaging was carried out by continuously scanning the same sample area using identical scan parameters and manually accounting for force drift.

Data analysis. Topography averages were calculated by using the Xmipp image processing package (Sorzano *et al*, 2004). Lattice parameters were defined using a 2D cross-correlation approach with the SEMPER image processing package (Saxton & Baumeister, 1982). All statistical analyses were carried out in IGOR Pro (Wavemetrics, Portland, OR, USA).

ACKNOWLEDGEMENTS

We are grateful to T. Gonen for preparing the initial lens membrane sample. This study was supported by the INSERM (Institut National de la Santé et Recherche Médicale) and INSERM Avenir, an ACI (Action Concertee Incitative) Nanosciences 2004 grant (to S.S.) and by the National Institutes of Health funding (to T.W.).

REFERENCES

Agre P (2004) Nobel lecture. Aquaporin water channels. *Biosci Rep* **24:** 127–163

Alcala J, Lieska N, Maisel H (1975) Protein composition of bovine lens cortical fiber cell membranes. *Exp Eye Res* **21:** 581–595

Binnig G, Quate CF, Gerber C (1986) Atomic force microscope. *Phys Rev Lett* **56:** 930–933

Chandy G, Zampighi GA, Kreman M, Hall JE (1997) Comparison of the water transporting properties of MIP and AQP1. *J Membr Biol* **159:** 29–39

Donaldson P, Kistler J, Mathias RT (2001) Molecular solutions to mammalian lens transparency. *News Physiol Sci* **16:** 118–123

Fleishman SJ, Unger VM, Yeager M, Ben-Tal NA (2004) Cα model for the transmembrane α helices of gap junction intercellular channels. *Mol Cell* **15:** 879–888

Fleschner CR, Cenedella RJ (1991) Lipid composition of lens plasma membrane fractions enriched in fiber junctions. *J Lipid Res* **32:** 45–53

Fotiadis D, Hasler L, Muller DJ, Stahlberg H, Kistler J, Engel A (2000) Surface tongue-and-groove contours on lens MIP facilitate cell-to-cell adherence. *J Mol Biol* **300:** 779–789

Giocondi MC, Le Grimellec C (2004) Temperature dependence of the surface topography in dimyristoylphosphatidylcholine/ distearoylphosphatidylcholine multibilayers. *Biophys J* **86:** 2218–2230

Gonen T, Sliz P, Kistler J, Cheng Y, Walz T (2004a) Aquaporin-0 membrane junctions reveal the structure of a closed water pore. *Nature* **13:** 193–197

Gonen T, Cheng Y, Kistler J, Walz T (2004b) Aquaporin-0 membrane junctions form upon proteolytic cleavage. *J Mol Biol* **342:** 1337–1345

Gonen T, Cheng Y, Sliz P, Hiroaki Y, Fujiyoshi Y, Harrison SC, Walz T (2005) Lipid–protein interactions in double-layered two-dimensional AQP0 crystals. *Nature* **438:** 633–638

Harries WE, Akhavan D, Miercke LJ, Khademi S, Stroud RM (2004) The channel architecture of aquaporin 0 at a 2.2-Å resolution. *Proc Natl Acad Sci USA* **101:** 14045–14050

Harris AL (2001) Emerging issues of connexin channels: biophysics fills the gap. *Quart Rev Biophys* **34:** 325–472

Hoh JH, Lal R, John SA, Revel JP, Arnsdorf MF (1991) Atomic force microscopy and dissection of gap junctions. *Science* **253:** 1405–1408

Jensen MO, Mouritsen OG (2004) Lipids do influence protein function—the hydrophobic matching hypothesis revisited. *Biochim Biophys Acta* **1666:** 205–226

Kistler J, Goldie K, Donaldson P, Engel A (1994) Reconstitution of native-type noncrystalline lens fibre gap junctions from isolated hemichannels. *J Cell Biol* **126:** 1047–1058

Kumar NM, Gilula NB (1996) The gap junction communication channel. *Cell* **84:** 381–388

Müller DJ, Fotiadis D, Scheuring S, Müller SA, Engel A (1999) Electrostatically balanced subnanometer imaging of biological specimens by atomic force microscopy. *Biophys J* **76:** 1101–1111

Saxton WO, Baumeister W (1982) The correlation averaging of a regularly arranged bacterial cell envelope protein. *J Microsc* **127:** 127–138

Scheuring S, Sturgis JN (2005) Chromatic adaptation of photosynthetic membranes. *Science* **309:** 484–487

Shiels A, Bassnett S (1996) Mutations in the founder of the MIP gene family underlie cataract development in the mouse. *Nat Genet* **12:** 212–215

Sorzano CO, Marabini R, Velazquez-Muriel J, Bilbao-Castro JR, Scheres SH, Carazo JM, Pascual-Montano A (2004) XMIPP: a new generation of an open-source image processing package for electron microscopy. *J Struct Biol* **148:** 194–204

Takemoto L, Takehana M, Horwitz J (1986) Covalent changes in MIP26K during aging of the human lens membrane. *Invest Ophthalmol Vis Sci* **27:** 443–446

Unger VM, Kumar NM, Gilula NB, Yeager M (1999) Three-dimensional structure of a recombinant gap junction membrane channel. *Science* **283:** 1176–1180

Yu XS, Yin X, Lafer EM, Jiang JX (2005) Developmental regulation of the direct interaction between the intracellular loop of connexin 45.6 and the C terminus of major intrinsic protein (aquaporin-0). *J Biol Chem* **280:** 22081–22090

Zampighi G, Simon SA, Robertson JD, McIntosh TJ, Costello MJ (1982) On the structural organization of isolated bovine lens fiber junctions. *J Cell Biol* **93:** 175–189

Zampighi GA, Eskandari S, Hall JE, Zampighi L, Kreman M (2002) Micro-domains of AQP0 in lens equatorial fibers. *Exp Eye Res* **75:** 505–519